International Journal of Cardiology 275 (2019) 120–128

Contents lists available at ScienceDirect

International Journal of Cardiology

journal homepage: www.elsevier.com/locate/ijcard

LRP5 controls cardiac QT interval by modulating the metabolic homeostasis of L-type calcium channel☆

Dandan Liang [a,b,1], Yahan Wu [a,b,1], Liping Zhou [a,b,1], Yongli Chen [a,d], Hongyu Liu [a,b], Duanyang Xie [a,b], Jian Huang [a,b], Yangyang Zhang [a,b], Yi Liu [a,b], Weidong Zhu [a,e], Jun Li [a,b,c,*], Yi-Han Chen [a,b,c,e,*]

[a] Key Laboratory of Arrhythmias of the Ministry of Education of China, East Hospital, Tongji University School of Medicine, Shanghai 200120, China
[b] Institute of Medical Genetics, Tongji University, Shanghai 200092, China
[c] Department of Cardiology, East Hospital, Tongji University School of Medicine, Shanghai 200120, China
[d] Dalian Medical University, Dalian 116044, China
[e] Department of Pathology and Pathophysiology, Tongji University School of Medicine, Shanghai 200092, China

ARTICLE INFO

Article history:
Received 18 October 2017
Received in revised form 4 June 2018
Accepted 6 June 2018
Available online 8 June 2018

Keywords:
Low-density lipoprotein receptor-related protein
QT interval
Action potential duration
Myocyte
L-type calcium channel
Proteasomal degradation

ABSTRACT

Background: Low-density lipoprotein receptor-related protein 5 (LRP5) has been intensively studied as a co-receptor for β-catenin-dependent Wnt signaling. Emerging evidences have demonstrated β-catenin-independent functions of LRP5. However, the biological role of LRP5 in the mammalian heart is largely unknown.
Methods and results: Conditional cardiac-specific *Lrp5* knockout (*Lrp5*-CKO) mice were generated by crossing *Lrp5*$^{flox/flox}$ mice with α*MHC*/MerCreMer mice. *Lrp5*-CKO mice consistently displayed normal cardiac structure and function. Telemetric electrocardiogram recordings revealed a short QT interval in *Lrp5*-CKO mice, which was tightly linked to the striking abbreviation of action potential duration (APD) in ventricular myocytes. The analysis of whole-cell currents indicated that a reduction in activity and protein expression of L-type calcium channel (LTCC), rather than other ion channels, contributed to the abnormality in APD. Furthermore, we showed that *Lrp5* ablation induced a significant convergence of $Ca_V1.2\alpha1c$ proteins to the endoplasmic reticulum. Consequently, increased proteasomal degradation of these proteins was observed, which was independent of the Wnt/β-catenin signaling pathway.
Conclusions: LRP5 directly modulates the degradation of LTCC to control cardiac QT interval. These findings provide compelling evidence for the potential role of LRPs in cardiac electrophysiology.

1. Introduction

The β-catenin-dependent Wnt signaling pathway mediates a myriad of biological process in both embryonic development and adult growth in mammals. Abnormalities in Wnt signaling have been linked to a wide range of pathologies in humans [1–3]. Low-density lipoprotein receptor-related proteins 5 and 6 (LRP5 and LRP6) serve as Wnt co-receptors for the canonical β-catenin pathway. Under pathophysiological conditions, LRP5/6 play critical roles in skeletal remodeling, osteoporosis pathogenesis and cancer formation [4, 5] and differentially mediate the response of the heart to ischemic insults [6] making LRP5/6 promising therapeutic targets for cardiac diseases.

As a critical Wnt co-receptor, LRP5 is highly homologous to LRP6 with key functions in canonical Wnt signaling. It was initially identified to recognize lipoproteins and protein ligands and subsequently mediate their endocytosis [5]. LRP5 also has β-catenin-independent functions. Morpholino-based knockdown of *Lrp5* in *Xenopus* embryos caused convergent extension and heart phenotypes, which were rescued by downregulation of noncanonical XWnt5a and XWnt11, suggesting that LRP5 regulates *Xenopus* development via inhibiting the noncanonical Wnt signaling [7]. Additionally, mutations of LRP5 have been implicated in the development of several human diseases. Loss-of-function mutations in the *Lrp5* gene were linked to osteoporosis pseudoglioma syndrome, developmental anomalies of eyes and cardiac valve disease [8, 9]. However, the biological roles of LRP5 in the mammalian heart remain poorly understood. Our recent study demonstrated that LRP6 regulates the assembly of cardiac gap junction and controls cardiac arrhythmic vulnerability in mice [10], suggesting an important role of LRP6 in cardiac electrophysiological homeostasis. Whether and how LRP5 plays in cardiac electric activity remain to be delineated.

The rhythmic electromechanical function of the heart depends on the generation and propagation of action potential (AP), which derives

☆ These authors take responsibility for all aspects of the reliability and freedom from bias of the data presented and their discussed interpretation.

* Corresponding authors at: Key Laboratory of Arrhythmias of the Ministry of Education of China, East Hospital, Tongji University School of Medicine, No. 150 Jimo Road, Shanghai 200120, China.
E-mail addresses: junli@tongji.edu.cn, (J. Li), yihanchen@tongji.edu.cn (Y.-H. Chen).
[1] These authors contributed equally to this work.

https://doi.org/10.1016/j.ijcard.2018.06.029
0167-5273/

from the sequential activation and inactivation of ion channels that conduct depolarizing and repolarizing currents. The QT interval of the surface electrocardiogram (ECG) is the time from the start of the Q wave to the end of the T wave, and reflects the ventricular action potential duration (APD) [11]. An abnormal QT interval, for instance, the long- or short-QT syndrome, is a marker for the potential of ventricular tachyarrhythmias like torsades de pointes and a risk factor for sudden death [12]. Here, we found that the ablation of *Lrp5* in cardiomyocytes induced the shortening of the QT interval without any effect on PR interval, RR interval or QRS waves. The increased degradation of L-type calcium channel (LTCC) protein through the ubiquitin-proteasome pathway should well accounts for the acceleration of cardiac repolarization and shortening of QT interval, and this was independent of Wnt/β-catenin signaling. The present findings reveal a critical role of LRP5 in cardiac electrophysiology.

2. Methods

2.1. Animal

This study conformed to the rules of the Guide for the Care and Use of Laboratory Animals made by the U.S. National Institutes of Health (National Academies Press; 2011) and the policies of the Animal Care and Use Committee of Tongji University School of Medicine.

2.2. Generation of conditional cardiac-specific Lrp5-knockout mice

The cardiac myocyte-specific *Lrp5* knockout (*Lrp5*-CKO) mice line was generated by crossing $Lrp5^{flox/flox}$ mice with αMHC/MerCreMer ($Cre^{+/-}$) mice. The mice were maintained with a mixed C57BL genetic background. To induce the specific deletion of the *Lrp5* gene in cardiomyocytes, the 2-month-old αMHC/MerCreMer; $Lrp5^{flox/flox}$ male mice were treated with tamoxifen (T5648, Sigma) via intraperitoneal injection (80 mg/kg, once a day for 5 consecutive days). All experiments in *Lrp5*-CKO mice were performed at the fourth week after the first tamoxifen exposure.

2.3. Telemetric recordings and analysis of ECG

For telemetric ECG recordings, the animals were anesthetized with 1–2% isoflurane anesthesia with spontaneous ventilation. A midline incision was made on the abdomen to insert a telemetric transmitter (ETA F20, Data Sciences International) into the subcutaneous skin, with paired wire electrodes placed over the thorax. Then the mice were housed in the single cage and exposed in 12 h dark/light cycle environment. The monitor of ECG was initiated at least 3 days after recovery from surgical implantation. ECG parameters were recorded using a telemetric receiver and an analog-to-digital conversion data acquisition system for display and analysis by AD Instruments LabChart 7 system [13]. ECG recordings were assessed by a skilled technician blinded to animal genotypes. The RR interval was measured as the duration between the peaks of two consecutive P waves. The QRS duration was detected from the onset of the Q wave to the inflection in the upstroke of the S wave. The QT interval was the duration between the beginning of the QRS complex and where the T wave returned to the isoelectric TP baseline. The abnormal complexes caused by physical activity were not analyzed [13]. All data were obtained from each mouse over a 24-h period.

2.4. Isolation of adult mice ventricular myocytes

The mice were injected with 200 μl heparin (100 IU/mouse) and anesthetized with pentobarbital (70 mg/kg). The heart was removed and perfused with a Ca^{2+}-free Krebs-Henseleit bicarbonate buffer before being Langendorff-perfused with Krebs-Henseleit bicarbonate buffer [14]. The detailed method was described in Supplementary materials.

2.5. Cardiomyocyte electrophysiology analysis

Whole-cell patch clamping technique was applied for ionic currents at room temperature (22–25 °C) and AP recording at 33 °C. Ionic currents were recorded with a whole cell recording configuration in voltage clamp mode, and APs were recorded with a whole cell recording configuration in current clamp mode. Borosilicate-glass electrodes had tip resistance between 2 and 5 MΩ. Current is expressed as current density (normalized to cell capacitance) [15]. Ventricular myocytes isolated from three to five sex-matched mice per genotype were employed in each cellular experiment.

2.6. Immunoprecipitation analysis

Tissues or cells were lysed in RIPA Buffer (Beyotime), supplemented with protease and phosphatase inhibitors. The lysate supernatant was collected after centrifugation (10 min at 10, 000 g, 4 °C). For immunoprecipitation, the lysates were incubated with $Ca_V1.2$ antibody (ACC-003, Alomone), LRP5 antibody (D80F2, CST) or isotype control immunoglobulin G (I8140, Sigma) overnight under continuous rotation at 4 °C. Next, the lysate-antibody mixtures were incubated with protein A–Sepharose beads (p2012, Beyotime) for 4 h at 4 °C. After incubation, the beads-antibody complexes were washed 5 times with PBS buffer (4000 g, 5 min, 4 °C). The samples were then analyzed by Western blot.

2.7. Immunofluorescence

Cells were fixed with 4% paraformaldehyde (PFA) (Sigma) for 15 min, washed twice with PBS for 5 min, and then permeabilized with 0.1% TritonX-100 for 10 min at room temperature. This was followed by 1 h of blocking of non-specific sites in 5% normal goat serum at room temperature. The cells then were then incubated with the primary antibodies: LRP5 (1:100, ab36121, Abcam), $Ca_v1.2α1c$ (1:100, ACC-003, Alomone) and PDI (1:100, NB300–517, Novus) at 4 °C overnight. The cells were then washed with PBST and incubated with the respective secondary antibodies conjugated to Alexa Fluor 488/555/647 (1:200, Invitrogen). Nuclear staining was performed with To-Pro 3 (Invitrogen) for 30 min if needed. The images were captured using a laser confocal scanning microscope (Leica).

2.8. Western blot

Tissue and cells were harvested and lysed with RIPA buffer (Beyotime) for protein extraction according to the manufacturer's instructions. Proteinase inhibitors (Roche) were used to minimize protein decomposition. The lysates were heated to 95 °C for 5 min, separated by NuPAGE 10% Bis-Tris Gels (Invitrogen) followed by the blotting of proteins onto a polyvinylidene fluoride (PVDF) membrane. The membranes were then blocked and incubated with the appropriate primary antibodies. The secondary antibodies conjugated to infrared dyes (Li-Cor) were applied to detect the specific bands. The labeled bands were visualized using an Odyssey imager. Western blots were quantified by densitometry using ImageJ software (NIH).

2.9. Quantitative PCR

Total RNA was extracted from ventricular tissues or cells using Trizol reagent (Ambion) according to the manufacturer's instructions. The cDNA was synthesized using PrimeScript™ RT reagent kit (Takara). Quantitative PCR was performed using specific sets of primers and SYBR Green Master Mix (Applied Biosystems Life Technologies). GAPDH levels were used to normalize the gene-specific expression levels. The primer sequences were listed in Supplementary table 2.

2.10. Statistical analysis

All statistical data are shown as the mean ± standard error of the mean (s.e.m.). Unpaired two-tailed Student's *t*-test and one-way ANOVA followed by Turkey's post-hoc test were used for the statistical comparison of two and more than two groups, respectively. Statistical analyses were performed using Prism 5.0 (GraphPad Software). A value of $P < 0.05$ was considered to be statistically significant.

3. Results

3.1. Cardiac-specific knockout of Lrp5 induces a shortened QT interval in adult mice

To analyze the roles of LRP5 in cardiac physiology, we generated an inducible cardiomyocyte-specific *Lrp5* knockout (*Lrp5*-CKO) mouse line. $Lrp5^{flox/flox}$ mice were crossed with MerCreMer(*Cre*) animals under the α-myosin heavy chain promoter (α-*MHC*) to allow the tamoxifen-dependent deletion of *Lrp5* in cardiomyocytes (Fig. 1A). Following tamoxifen administration, the LRP5 protein was significantly reduced in *Lrp5*-CKO hearts (Fig. 1B). The loss of *Lrp5* had no effects on cardiac function and structure, as demonstrated by the normal ejection fraction, fractional shortening, left ventricular posterior wall thickness (diastole), inter ventricular septum thickness (diastole), left ventricular internal dimension (diastole), heart morphology, myocardial fibrosis and cardiomyocyte size (Fig. S1 and 2). Collectively, LRP5 is dispensable for the maintenance of cardiac structure and mechanical function.

Next, using an implantable telemetry system, we monitored the cardiac electrophysiology in *Lrp5*-CKO mice over a 24-h period under conscious conditions. We found that the variability in heart rate and QT interval was low across animals and over time in both *Lrp5*-CKO mice and littermate normal controls (Fig. S3A and B). The PR interval, the RR interval and the QRS duration in *Lrp5*-CKO mice

were comparable to those in $Cre^{+/-}$ littermates. Unexpectedly, the QT interval was shortened by ~25% in *Lrp5*- CKO mice (Fig. 1: C to G), as well as the QTc interval (Fig. S4). These results suggest an important link between LRP5 and cardiac electrophysiological activities.

3.2. LRP5 deficit-induced QT shortening is attributable to accelerated repolarization of ventricular AP

QT interval is a reflection of ventricular action potential duration, and represents the time during which the ventricles depolarize and repolarize.

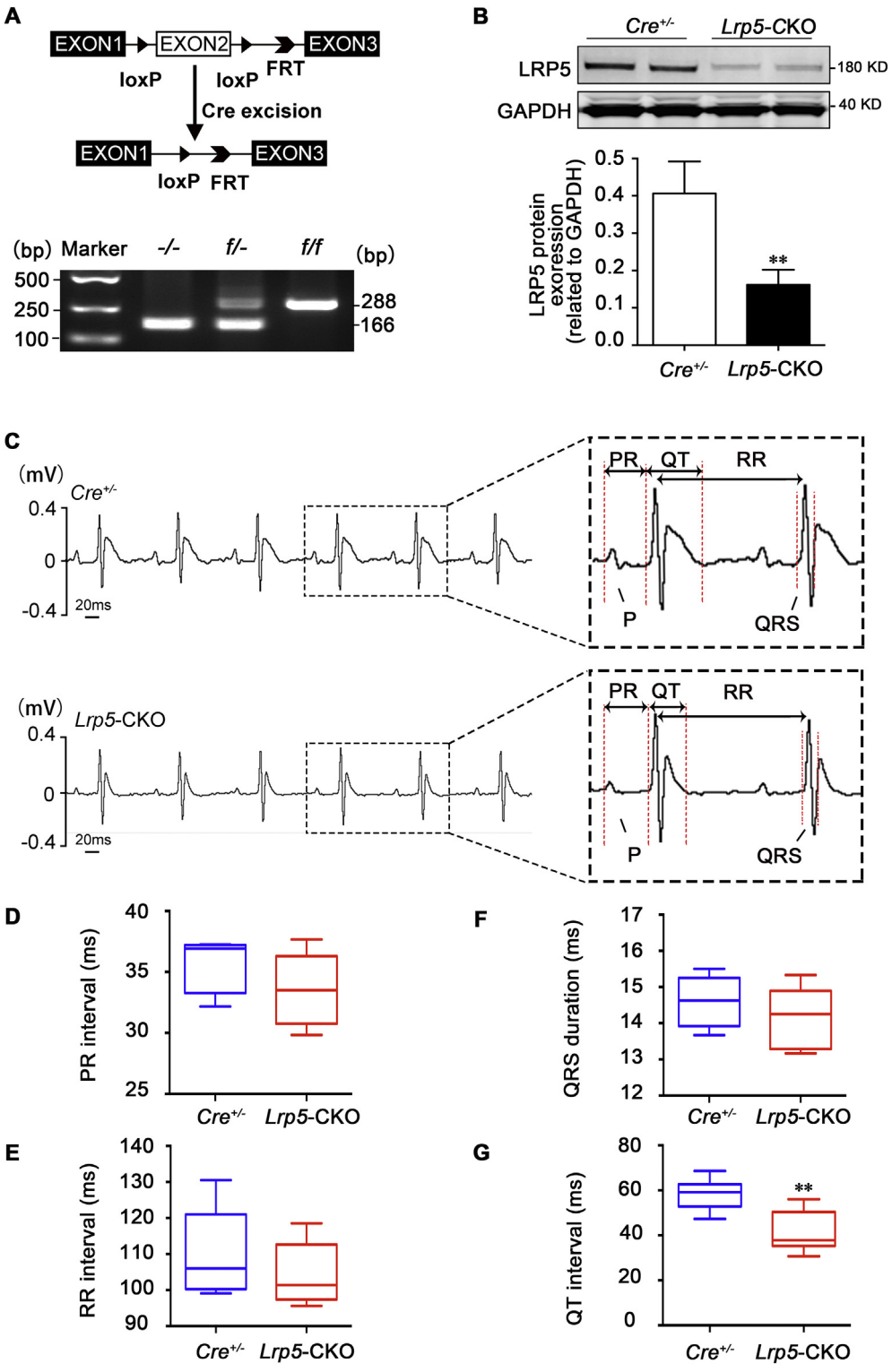

Fig. 1. Ablation of LRP5 shortens the QT interval in mice. (A) Generation of the mouse line with conditional cardiac-specific knockout of the *Lrp5* gene. Top, schematic depicting the targeting and genotyping strategies for the *Lrp5* floxed alleles. LoxP sites (arrowheads) and FRT sites (diamonds) are shown. After Cre-mediated DNA recombination, the LoxP-flanked *Lrp5* gene segment is excised. Bottom, Genotyping identification with the photograph of an agarose gel containing PCR amplimers for WT (−/−) and floxed (f/−; f/f) *Lrp5* alleles derived from genomic DNA of mice with different *Lrp5* genotypes. (B) Western blotting examination of LRP5 protein in heart tissues of *Lrp5*-CKO mice. Top, representative blots; bottom, pooled data. $n = 5$, n represents the number of animals. (C) Representative electrocardiograms in $Cre^{+/-}$ and *Lrp5*-CKO mice. (D–G) Summary of the analysis of ECG parameters (PR, RR, QRS, and QT). $Cre^{+/-}$mice: $n = 6$; *Lrp5*-CKO mice: $n = 6$. n represents the number of animals. Data are the mean ± s.e.m. $^{**}P < 0.01$.

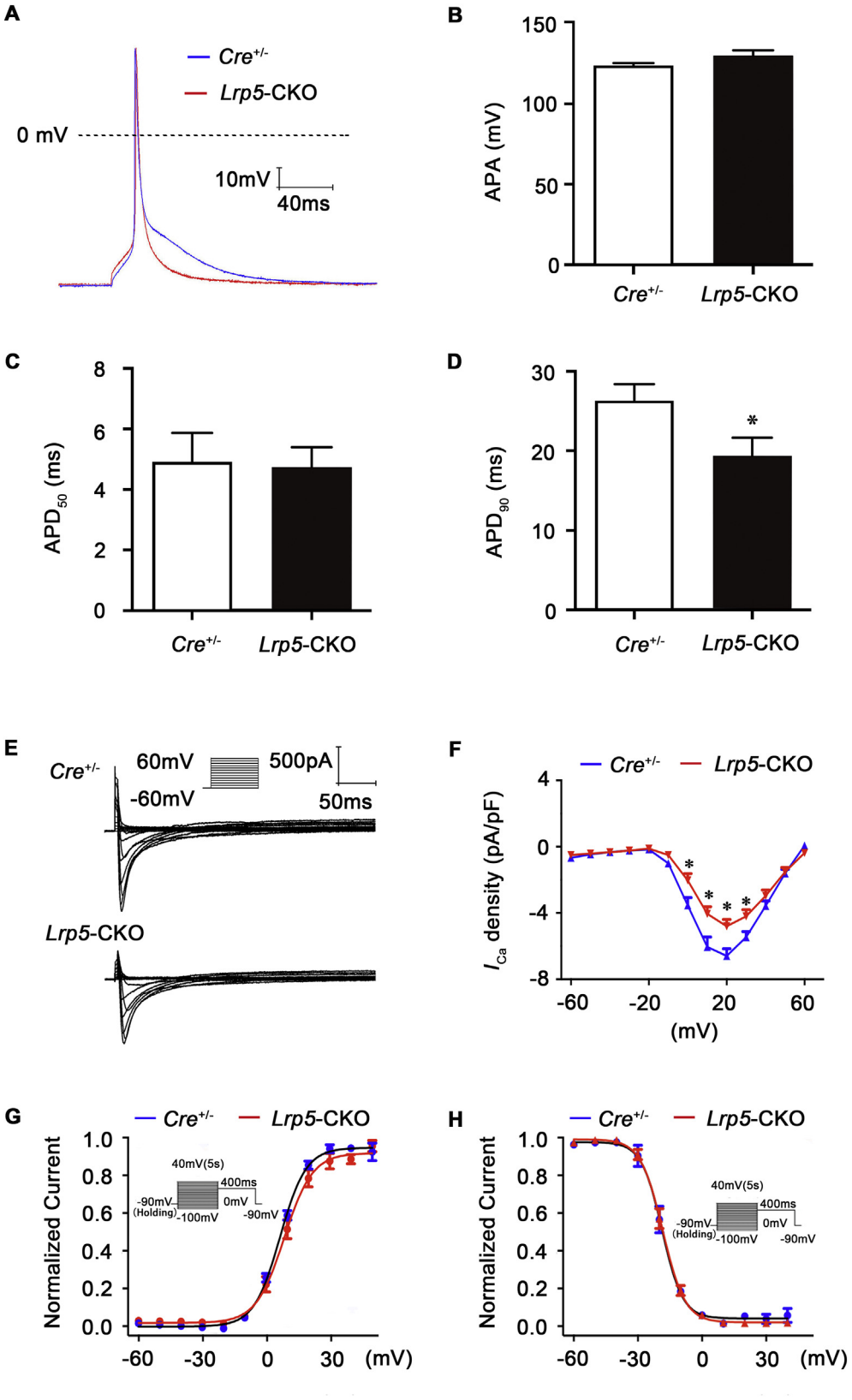

Fig. 2. LRP5 deficiency abbreviates action potential duration (APD) and depresses $I_{Ca,L}$ in mouse ventricular myocytes. (A) Representative AP traces of ventricular myocytes from $Cre^{+/-}$ and *Lrp5*-CKO mice. (B-D) Summary data of AP amplitude (APA) and APD at 50% and 90% repolarization from $Cre^{+/-}$ and *Lrp5*-CKO mice. ($n = 17$ for $Cre^{+/-}$, $n = 19$ for *Lrp5*-CKO). (E) Representative traces of L-type calcium channel current ($I_{Ca,L}$) in single ventricular myocytes of $Cre^{+/-}$ and *Lrp5*-CKO mice. (F) Analysis of the I–V relationship for $I_{Ca,L}$ currents. (G-H) Measurement of the activation (G) and inactivation (H) curves for $I_{Ca,L}$ currents. $Cre^{+/-}$ mice: $n = 10$; *Lrp5*-CKO mice: $n = 9$. (As reported previously, Li et al., 2017), $I_{Ca,L}$ currents are mainly associated with APD_{90} rather than APD_{50} in the ventricular myocytes of adult mice). APD_{50} and APD_{90}, action potential duration at 50% and 90% repolarization, respectively. Data are the mean ± s.e.m. $^*P < 0.05$, n represents the number of myocytes.

To explore the cellular electrophysiological basis of the shortened QT interval in *Lrp5*-CKO mice, we examined the AP of freshly-isolated ventricular myocytes in the *Lrp5*-CKO mice and the $Cre^{+/-}$ littermates (Fig. 2A). The resting membrane potential was −74.2 ± 1.3 mV in $Cre^{+/-}$ cardiomyocytes and − 72.1 ± 1.8 mV in *Lrp5*-CKO cardiomyocytes. There were also no significant differences in AP amplitude between the two groups (Fig. 2B). However, the action potential duration (APD) was significantly shorter in *Lrp5*-CKO versus $Cre^{+/-}$ cardiomyocytes at 90% repolarization (APD_{90}), while the APD_{50} was not changed (Fig. 2C, D).

3.3. Reduction of $Ca_V1.2$ channel current underlies the abnormalities in AP repolarization

In the adult mouse ventricle, the formation of APs is mainly involved in I_{to} (transient outward potassium current), I_{k1} (inward rectifier potassium current), $I_{Ca,L}$ (LTCC) and I_{Na} (voltage-gated sodium channel current) [16, 17]. Hence, we examined these currents in *Lrp5*-CKO and $Cre^{+/-}$ cardiomyocytes. There were no significant differences in mean cell capacitance between the two groups (Fig. S5A). Depolarizing steps

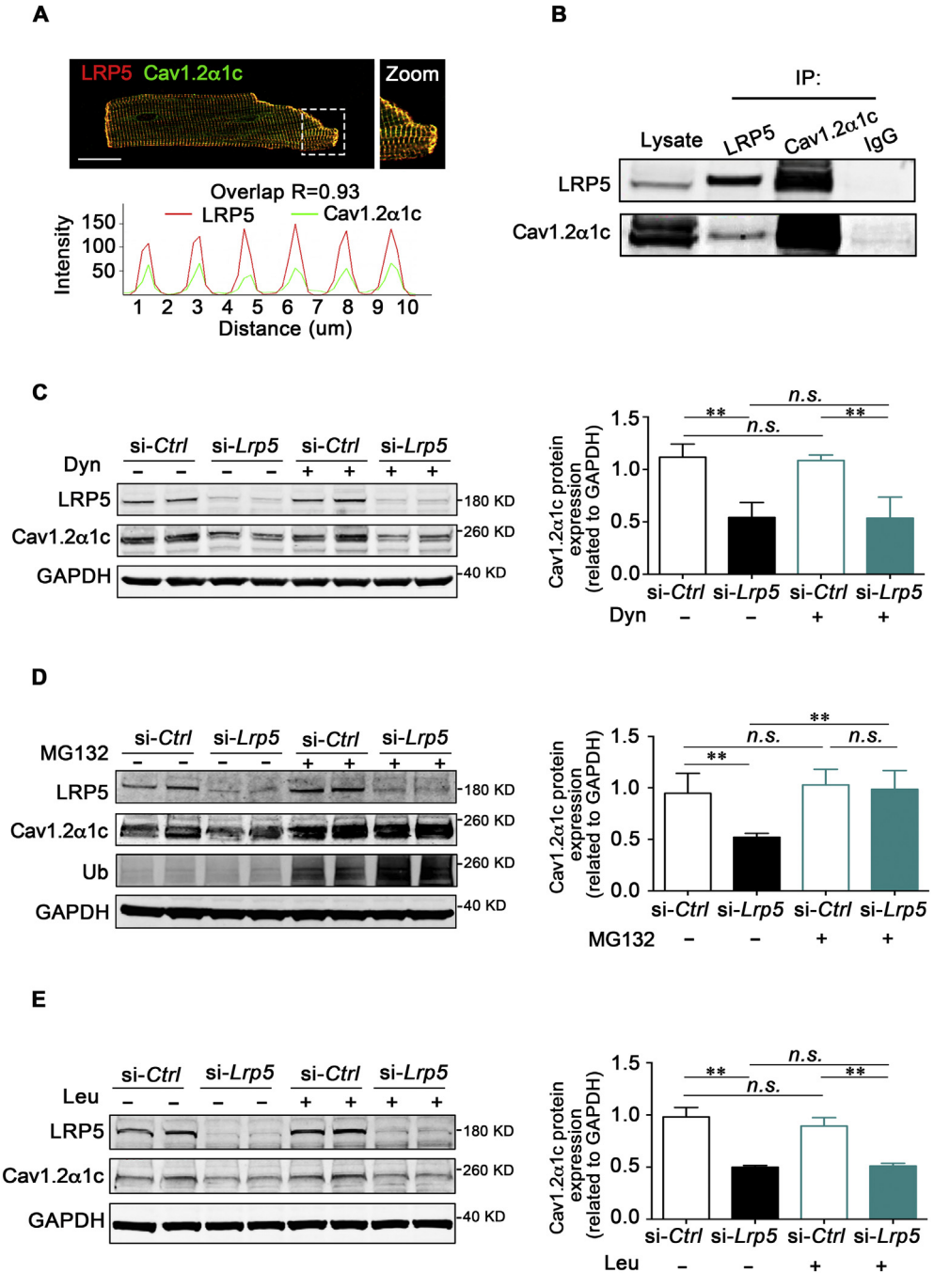

Fig. 3. LRP5 modulates the proteasomal degradation of $Ca_V1.2α1c$ protein. (A) Immunofluorescence staining of LRP5 and $Ca_V1.2α1c$ in intact adult mouse ventricular myocytes. Top, representative immunofluorescence imaging of endogenous LRP5 (red) and $Ca_V1.2α1c$ (green). Scale bar, 25 μm; bottom, quantitation of the normalized intensity versus normalized distance from LRP5 (red) and $Ca_V1.2α1c$ (green). (B) Co-immunoprecipitation of endogenous LRP5 and $Ca_V1.2α1c$ in adult mouse ventricular myocytes. (C) The protein expression of $Ca_V1.2α1c$ in *Lrp5*-deficient NRVMs treated with dynasore (Dyn) for 48 h. Dyn was used to inhibit dynamin activity. Left, typical blots; right, pooled data. (D) The effects of proteasome inhibition on $Ca_V1.2α1c$ protein expression and $Ca_V1.2α1c$ ubiquitination in *Lrp5*-deficient NRVMs exposed to MG132 for 48 h. MG132, a proteasomal inhibitor. Left, typical blots; right, pooled data. (E) The effects of lysosome inhibition on $Ca_V1.2α1c$ protein expression in *Lrp5*-deficient NRVMs treated with leupeptin (Leu). Leu was used to inhibit lysosome degradation. Left, typical blots; right, pooled data. Data are the mean ± s.e.m. $^{**}P < 0.01$. $n = 3$, n represents the number of experiments. n.s.: non-significance.

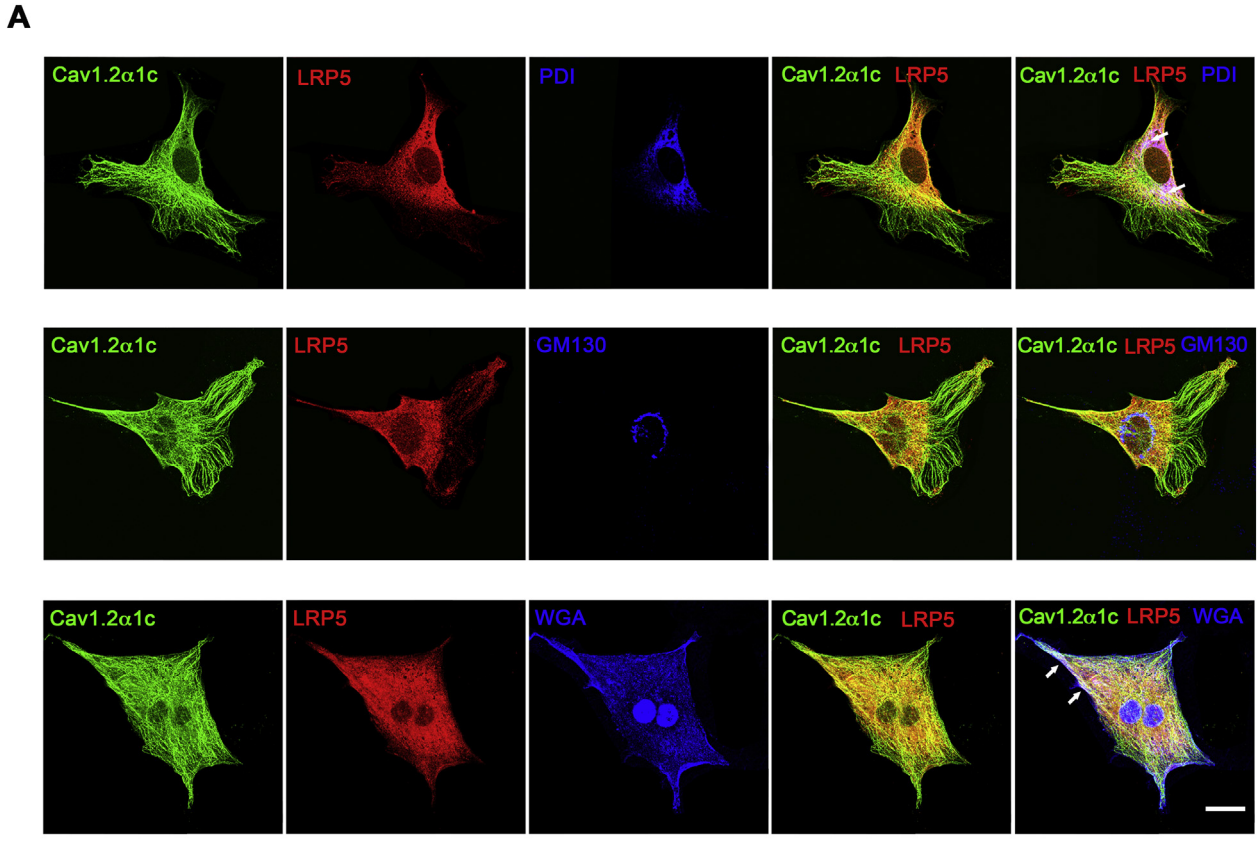
A
Cav1.2α1c
LRP5
PDI
Cav1.2α1c LRP5
Cav1.2α1c LRP5 PDI
Cav1.2α1c
LRP5
GM130
Cav1.2α1c LRP5
Cav1.2α1c LRP5 GM130
Cav1.2α1c
LRP5
WGA
Cav1.2α1c LRP5
Cav1.2α1c LRP5 WGA

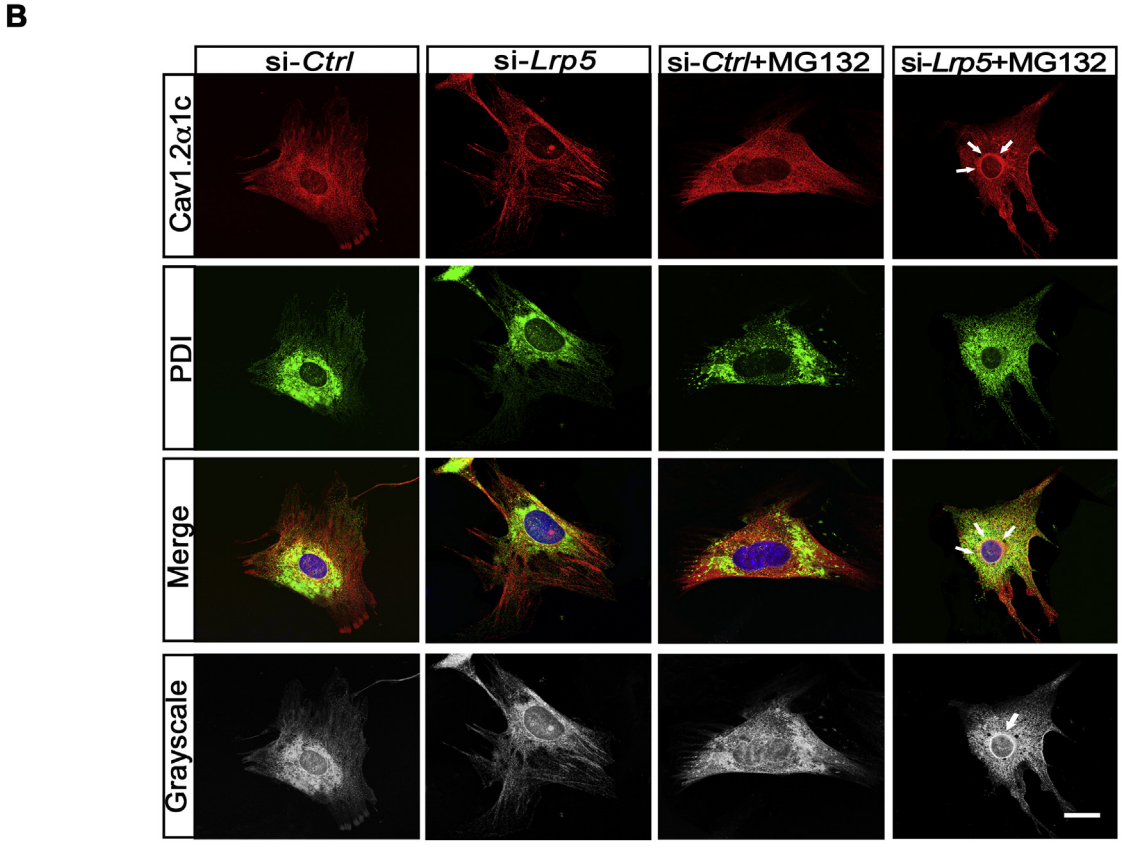
B
si-Ctrl
si-Lrp5
si-Ctrl+MG132
si-Lrp5+MG132
Cav1.2α1c
PDI
Merge
Grayscale

produced outward currents that rose rapidly to a peak and then decayed, and the maximal peak and the slow component of I_{to} were not significantly different in *Lrp5*-CKO cardiomyocytes relative to $Cre^{+/-}$ controls (Fig. S5: B to D). Moreover, the maximal I_{K1} currents elicited by hyperpolarizing pulses and the shape of the current-voltage relationship curves of I_{Na} were also similar in *Lrp5*-CKO and $Cre^{+/-}$ cardiomyocytes (Fig. S5: E to F). In contrast, there were significant differences between the two groups in $I_{Ca,L}$, with a reduction of $I_{Ca,L}$ density in *Lrp5*-CKO cardiomyocytes (Fig. 2: E to H). These results suggest that the depressed function of the LTCC contributes to the LRP5 deficiency-induced shortening of APD_{90} as above-mentioned. This finding was consistent with the previous report that $I_{Ca,L}$ currents are mainly associated with APD_{90} and have no significant effects on APD_{50} in ventricular myocytes of adult mice [18].

3.4. LRP5 regulates $Ca_V1.2$ expression in a β-catenin-independent manner

LTCC are multisubunit complexes formed by different isoforms of the pore forming α1 subunit named α1S (Cav1.1, in skeletal muscle), α1C (Cav1.2, in cardiac and smooth muscle), α1D (Cav1.3, in neuron and heart), and α1F (Cav1.4, in retina). The Cav1.2α1c expresses predominantly in adult mouse ventricular myocytes, and the Cav1.3α1d is functionally expressed in early embryonic mouse ventricular myocytes [19]. To gain insight into the mechanism by which LRP5 regulates $I_{Ca,L}$, the levels of $Ca_V1.2α1c$ protein were measured in *Lrp5*-CKO hearts. In contrast to the $Cre^{+/-}$ controls, the total amount of $Ca_V1.2α1c$ protein was markedly reduced in *Lrp5*-CKO mice (Fig. S6A), while $Ca_V1.3α1d$ protein expression was not changed (Fig. S7). Additionally, the total and fractional proteins of Na^+ channel and voltage-dependent K^+ channels in the hearts were also examined, and no significant differences were observed between the *Lrp5*-CKO and $Cre^{+/-}$ mice (Fig. S8). These evidences indicate that the reduced $Ca_V1.2α1c$ protein underlies the abnormality of $I_{Ca,L}$ induced by LRP5 deficiency.

LRP5 is best known as a Wnt co-receptor that facilitates Wnt signaling and subsequent to the cytoplasmic stabilization of β-catenin. The activation of Wnt signaling inactivates a multiprotein complex, including Axin2 and glycogen synthase kinase-3β (GSK-3β), which normally renders β-catenin unstable [20, 21]. To assess whether the LRP5-mediated regulation of $Ca_V1.2α1c$ was involved in the Wnt/β-catenin signaling pathway, the expression of β-catenin, Axin2 and GSK-3β were evaluated in the *Lrp5*-CKO heart tissues. *Lrp5* ablation did not change β-catenin expression, both in the cell nucleus and cytoplasm (Fig. S6B). The protein and mRNA expression of β-catenin, Axin2 and GSK-3β were also not significantly changed by *Lrp5* ablation (Fig. S6C, D). Moreover, the reduction in β-catenin did not affect $Ca_V1.2α1c$ protein expression in neonatal rat ventricular myocytes (NRVMs) (Fig. S6E). The expression of β-catenin, Axin2 and GSK-3β was also examined in *Lrp5*-knockdown NRVMs (Fig. S9). The results were consistent with those in *Lrp5*-CKO heart tissues. Collectively, these findings revealed that LRP5 regulated $Ca_V1.2α1c$ expression in β-catenin-independent pathway.

3.5. LRP5 post-transcriptionally modulates the expression of $Ca_V1.2α1c$

To investigate the potential mechanisms underlying the reduction of $Ca_V1.2α1c$ protein, its level of transcription was first examined. We found that the $Ca_V1.2α1c$ mRNA level was not changed in *Lrp5*-CKO hearts (Fig. S10A). Next, a luciferase reporter plasmid containing the $Ca_V1.2α1c$ promoter region was co-transfected with *Lrp5*-siRNA (si-*Lrp5*) or scrambled control (si-Ctrl) in NRVMs. As shown in Fig. S10B, LRP5 reduction did not affect the transcriptional activity of the calcium voltage-gated channel subunit alpha1C (*CACNA1c*) promoter, suggesting that LRP5 modulates $Ca_V1.2α1c$ protein expression post-transcriptionally.

3.6. LRP5 interacts directly with $Ca_V1.2α1c$ in adult cardiomyocytes

To assess whether LRP5 directly modulates $Ca_V1.2α1c$ expression, we detected the subcellular localization of LRP5 in isolated adult mice ventricular myocytes and examined whether LRP5 co-localized with $Ca_V1.2α1c$. We found that the distribution of LRP5 has a typical pattern that was similar to $Ca_V1.2α1c$. They overlapped significantly (Fig. 3A). Furthermore, co-immunoprecipitation experiments with the homogenate derived from mice ventricular tissues identified a physical interaction of LRP5 with $Ca_V1.2α1c$ (Fig. 3B). Additionally, the co-immunoprecipitation examination also showed that LRP5 co-precipitated with $Ca_V1.2α1c$ in NRVMs (Fig. S11A). These results revealed the direct binding of endogenous LRP5 to $Ca_V1.2α1c$ under physiological conditions.

LRP5 consists of a large extracellular domain containing four β-propellers plus EGF repeats, which are essential for its binding to Wnt and other ligands/antagonists, and three LDLR-A repeats. The cytoplasmic region of LRP5 contains five highly conserved PPPSPxS motifs that serve as Axin binding sites [5]. To identify the binding region of LRP5 with $Ca_V1.2α1c$, we generated *Lrp5* N-terminus and *Lrp5* C-terminus truncated mutants (*Lrp5*-NT△ and *Lrp5*-CT△, respectively) fused with a flag tag (Fig. S11B). LRP5-NT△ or LRP5-CT△ was then co-transfected with the $Ca_V1.2α1c$ plasmid into HEK293 cells, and as a result, LRP5-NT△ co-precipitated with $Ca_V1.2α1c$ (Fig. S11C, E). Moreover, we found that overexpression of N-terminus but not C-terminus truncated mutants greatly reconciled the downregulation of $Ca_V1.2α1c$ protein by *Lrp5* knockdown in NRVMs (Fig. S11D, F), suggesting that the C-terminal region is responsible for the functional binding of LRP5 to $Ca_V1.2α1c$.

3.7. LRP5 deficiency induces the retention of $Ca_V1.2α1c$ in the endoplasmic reticulum and subsequently its proteasomal degradation

Next, we measured the trafficking and/or degradation of the $Ca_V1.2α1c$ protein. Following modification at ER/Golgi complex, the $Ca_V1.2$ channel life cycle involves many processes, including the transport to the plasma membrane, movement within the membrane, internalization, and eventual degradation or possible recycling [22]. Using NRVMs transfected with adenovirus against *Lrp5* (ad-*Lrp5 shRNA*), we found that the expression and activity of $Ca_V1.2α1c$ protein, and no other channels, were significantly reduced (Fig. S12), which was consistent with its alteration in *Lrp5*-CKO mice.

To assess whether the endocytosis is involved in the reduction of $Ca_V1.2α1c$ expression, we exposed NRVMs to dynasore, a specific dynamin GTPase inhibitor that blocks endocytosis. Dynasore treatment failed to prevent the reduction of the $Ca_V1.2α1c$ protein in *Lrp5*-knockdown myocytes, precluding the contribution of membrane $Ca_V1.2$ channel endocytosis (Fig. 3C). The degradation of the $Ca_V1.2α1c$ protein was then examined. We treated NRVMs with the proteasomal inhibitor, MG132, or the lysosomal inhibitor, leupeptin, after transfection with si-*Lrp5* or si-Ctrl. Proteasomal inhibition rescued the reduction of $Ca_V1.2α1c$ protein expression, whereas lysosome inhibition had no effect, indicating that LRP5 deficiency reduced $Ca_V1.2α1c$ protein expression by promoting the proteasomal degradation of the channel (Fig. 3D, E). Since the ubiquitination of $Ca_V1.2α1c$ is a critical step in the proteasome-mediated protein

Fig. 4. LRP5 deficiency induces the retention of $Ca_V1.2α1c$ in the endoplasmic reticulum. (A) Immunofluorescence imaging of the co-localization of $Ca_V1.2α1c$ with LRP5 at the membrane, ER and Golgi apparatus. PDI, an ER marker protein; GM130, a Golgi marker protein; WGA: wheat germ agglutinin. White arrows indicated the colocation of Cav1.2α1c and LRP5 at the ER and membrane surface. Scale bar, 20 μm. (B) Imaging of the co-localization of $Ca_V1.2α1c$ and ER in *Lrp5*-deficient neonatal rat ventricular myocytes. White arrows indicated the retention of $Ca_V1.2α1c$ in the ER. Scale bar, 20 μm.

degradation pathway, we also assessed this process. The results showed that *Lrp5* knockdown increased the ubiquitination of $Ca_V1.2\alpha1c$ protein (Fig. 3D). In addition, immunofluorescence experiment revealed that LRP5 partially co-localized with $Ca_V1.2\alpha1c$ both in the ER and on the membrane surface in intact cultured NRVMs (Fig. 4A), and *Lrp5* knockdown induced the convergence of $Ca_V1.2\alpha1c$ in the ER (Fig. 4B), suggesting that LRP5 might be involved in handling of the $Ca_V1.2\alpha1c$ protein within ER. Taken together, our findings provided evidence that LRP5 regulates $Ca_V1.2\alpha1c$ expression by modulating the proteasome degradation process.

4. Discussion

These findings uncovered the importance of LRP5 in cardiac electrophysiological homeostasis. First, LRP5 inactivation shortened the QT interval. Second, APD was strikingly abbreviated in *Lrp5*-CKO ventricular myocytes. Third, the reduction of $I_{Ca,L}$ density is responsible for APD abbreviation underlying the shortened QT interval. Finally, LRP5 defects induced the ubiquitin-proteasomal degradation of $Ca_V1.2\alpha1c$ independently of the Wnt/β-catenin signaling pathway.

LRP5 plays an essential role in bone development, eye vascularization, cholesterol metabolism, and the modulation of glucose-induced insulin secretion, in which it acts as a Wnt co-receptor that transduces Wnt signaling via the canonical pathway [8, 23]. As LRP5 plays a critical role in transducing signals from Wnt ligands, previous studies on LRP5 have mainly focused on the Wnt/β-catenin pathway [5]. Unexpectedly, we found that LRP5 deficiency led to the shortening of the QT interval in vivo, without any effect on Wnt signaling. These findings suggest that LRP5 has tissue-specific functions, and performs distinct roles in the heart.

LTCCs are essential for the electrical and mechanical properties of the heart. Missense mutations in genes encoding cardiac $Ca_V1.2$ subunits induce the loss-of-function of $I_{Ca,L,}$ which underlie the short QT interval in patients [24, 25]. This is similar to the phenotype observed in *Lrp5*-CKO mice. We revealed that LRP5 deficiency increased the ubiquitination and proteasomal degradation of $Ca_V1.2\alpha1c$. Protein expression is governed through three fundamental processes including protein synthesis, trafficking, recycle, internalization and degradation [26]. In view of the significant convergence of $Ca_V1.2\alpha1c$ at the ER of *Lrp5*-deficient cardiomyocytes exposed to MG132, it seems plausible that *Lrp5* deficiency leaded to the misfolding and misassembly of the $Ca_V1.2\alpha1c$ protein in the ER. However, the molecular details regarding LRP5-mediated regulation of $Ca_V1.2\alpha1c$ expression remain to be defined.

In addition to its role in AP, the influx of Ca^{2+} from LTCCs is also involved in intracellular signaling and the regulation of the expression of genes that are involved in cardiac hypertrophy and pathological remodeling [27–29]. As previously reported, a decrease in $I_{Ca,L}$ currents was observed in cardiomyocytes from failing human hearts or animal models of heart failure [30, 31]. Adult cardiomyocytes from the hearts of $\alpha1C^{-/+}$ mice at 10 weeks of age showed a decrease in $I_{Ca,L}$ currents and a modest decrease in cardiac function, which were not observed at 3 weeks [32]. These data suggest that the contractility of the progressively failing heart was affected by numerous factors, besides the altered Ca^{2+} channel, and may account for the normal cardiac structure and function despite the depressed LTCC activity in *Lrp5*-CKO mice.

LRP5 and LRP6 are highly homologous proteins with similar biological roles in canonical Wnt signaling [3, 5]. Recently, we reported the scaffold function of LRP6 in the formation of gap junctions between cardiomyocytes. Interestingly, the *Lrp6*-CKO mice displayed a normal QT interval in our study [10]. The differential phenotype of LRP6 and LRP5 in cardiac repolarization revealed that LRP5 has a distinctive feature in regulating cardiac electrophysiology.

In conclusion, we provide direct evidence for the role of LRP5 in the maintenance of cardiac QT interval. LRP5 deficiency promotes ubiquitin-proteasomal degradation of the ion channel proteins and leads to the dyshomeostasis of cardiac electric activity. Given that abnormalities in QT interval have been associated with lethal cardiac arrhythmias, LRP5 may act as a potential interventional target for the relevant heart disease.

Competing interests

The authors have declared that no competing interests exist.

Acknowledgements

This work was funded by the Key Program of National Natural Science Foundation of China (81530017, to Yi-Han Chen), the National Innovative Research Groups Program of the National Natural Science Foundation of China (81521061, to Yi-Han Chen), the General Program of the National Natural Science Foundation of China (81770397, to Yi-Han Chen; 81670360, to Jun Li; 81500252, 81770267, to Dandan Liang), the Fundamental Research Funds for the Central Universities (1500219135, to Yi-Han Chen; 1507219086, to Dandan Liang), the Outstanding Young Talent Training Program of Shanghai Municipal Commission of Health and Family Planning (2017YQ045, to Dandan Liang).

Appendix A. Supplementary data

Supplementary data to this article can be found online at https://doi.org/10.1016/j.ijcard.2018.06.029.

References

[1] R.T. Moon, A.D. Kohn, G.V. De Ferrari, A. Kaykas, WNT and beta-catenin signalling: diseases and therapies, Nat. Rev. Genet. 5 (2004) 691–701.
[2] R. Baron, M. Kneissel, WNT signaling in bone homeostasis and disease: from human mutations to treatments, Nat. Med. 19 (2013) 179–192.
[3] B.T. MacDonald, K. Tamai, X. He, Wnt/beta-catenin signaling: components, mechanisms, and diseases, Dev. Cell 17 (2009) 9–26.
[4] K.I. Pinson, J. Brennan, S. Monkley, B.J. Avery, W.C. Skarnes, An LDL-receptor-related protein mediates Wnt signalling in mice, Nature 407 (2000) 535–538.
[5] D.M. Joiner, J. Ke, Z. Zhong, Xu He, B.O. Williams, LRP5 and LRP6 in development and disease, Trends Endocrinol. Metab. 24 (2013) 31–39.
[6] D. Wo, J. Peng, D.N. Ren, et al., Opposing roles of Wnt inhibitors IGFBP-4 and Dkk1 in cardiac ischemia by differential targeting of LRP5/6 and β-catenin, Circulation 134 (2016) 1991–2007.
[7] V. Bryja, E.R. Andersson, A. Schambony, et al., The extracellular domain of Lrp5/6 inhibits noncanonical Wnt signaling in vivo, Mol. Biol. Cell 20 (2009) 924–936.
[8] Y. Gong, R.B. Slee, N. Fukai, et al., LDL receptor-related protein 5 (LRP5) affects bone accrual and eye development, Cell 107 (2001) 513–523.
[9] N.M. Rajamannan, The role of Lrp5/6 in cardiac valve disease: LDL-density-pressure theory, J. Cell. Biochem. 112 (2011) 2222–2229.
[10] J. Li, C. Li, D. Liang, et al., LRP6 acts as a scaffold protein in cardiac gap junction assembly, Nat. Commun. 7 (2016), 11775. .
[11] E. Marbán, Cardiac channelopathies, Nature 415 (2002) 213–218.
[12] A.R. Daisy, Q.D. George, The promise of induced pluripotent stem cells in research and therapy, Nature 481 (2012) 295–305.
[13] G.F. Mitchell, A. Jeron, G. Koren, Measurement of heart rate and QT interval in the conscious mouse, Am. J. Phys. 274 (1998) H747–H751.
[14] K. Wei, V. Serpooshan, C. Hurtado, et al., Epicardial FSTL1 reconstitution regenerates the adult mammalian heart, Nature 525 (2015) 479–485.
[15] J. Li, D. Xie, J. Huang, et al., Cold-inducible RNA-binding protein regulates cardiac repolarization by targeting transient outward potassium channels, Circ. Res. 116 (2015) 1655–1659.
[16] J.M. Nerbonne, R.S. Kass, Molecular physiology of cardiac repolarization, Physiol. Rev. 85 (2005) 1205–1253.
[17] N. Schmitt, M. Grunnet, S.P. Olesen, Cardiac potassium channel subtypes: new roles in repolarization and arrhythmia, Physiol. Rev. 94 (2014) 609–653.
[18] G. Li, J. Wang, P. Liao, et al., Exclusion of alternative exon 33 of Cav1.2 calcium channels in heart is proarrhythmogenic, Proc. Natl. Acad. Sci. U. S. A. 114 (2017) E4288–E4295.
[19] H. Takemura, K. Yasui, T. Opthof, et al., Subtype switching of L-type Ca^{2+} channel from Cav1.3 to Cav1.2 in embryonic murine ventricle, Circ. J. 69 (2005) 1405–1411.
[20] B.T. MacDonald, X. He, Frizzled and LRP5/6 receptors for Wnt/β-catenin signaling, Cold Spring Harb. Perspect. Biol. 4 (2012) (pii: a007880).
[21] V.S. Li, S.S. Ng, P.J. Boersema, et al., Wnt signaling through inhibition of β-catenin degradation in an intact Axin1 complex, Cell 149 (2012) 1245–1256.
[22] C. Altier, A. Garcia-Caballero, B. Simms, et al., The Cavβ subunit prevents RFP2-mediated ubiquitination and proteasomal degradation of L-type channels, Nat. Neurosci. 14 (2011) 173–180.

[23] T. Fujino, H. Asaba, M.J. Kang, et al., Low-density lipoprotein receptor-related protein 5 (LRP5) is essential for normal cholesterol metabolism and glucose-induced insulin secretion, Proc. Natl. Acad. Sci. U. S. A. 100 (2003) 229–234.
[24] C. Antzelevitch, G.D. Pollevick, J.M. Cordeiro, et al., Loss-off function mutations in the cardiac calcium channel underlie a new clinical entity characterized by ST segment elevation, short QT intervals, and sudden cardiac death, Circulation 115 (2007) 442–449.
[25] C. Patel, G.X. Yan, C. Antzelevitch, Short QT syndrome: from bench to bedside, Circ. Arrhythm. Electrophysiol. 3 (2010) 401–408.
[26] K. Römisch, Endoplasmic reticulum-associated degradation, Annu. Rev. Cell Dev. Biol. 21 (2005) 435–456.
[27] X.H. Wehrens, S.E. Lehnart, A.R. Marks, Intracellular calcium release and cardiac disease, Annu. Rev. Physiol. 67 (2005) 69–98.
[28] H. Nakayama, X. Chen, C.P. Baines, et al., Ca^{2+}- and mitochondrial-dependent cardiomyocyte necrosis as a primary mediator of heart failure, J. Clin. Invest. 117 (2007) 2431–2444.
[29] F. Hofmann, V. Flockerzi, S. Kahl, J.W. Wegener, L-type Cav1.2 calcium channels: fromin vitro findings to in vivo function, Physiol. Rev. 94 (2014) 303–326.
[30] S. Richard, F. Leclercq, S. Lemaire, C. Piot, J. Nargeot, Ca^{2+} currents in compensated hypertrophy and heart failure, Cardiovasc. Res. 37 (1998) 300–311.
[31] X. Chen, V. Piacentino 3rd, S. Furukawa, B. Goldman, K.B. Margulies, S.R. Houser, L-type Ca^{2+} channel density and regulation are altered in failing human ventricular myocytes and recover after support with mechanical assist devices, Circ. Res. 91 (2002) 517–524.
[32] S.A. Goonasekera, K. Hammer, M. Auger-Messier, et al., Decreased cardiac L-type Ca^{2+} channel activity induces hypertrophy and heart failure in mice, J. Clin. Invest. 122 (2012) 280–290.